RESEARCH ARTICLE

EVOLUTIONARY ECOLOGY

Metabolic scaling is the product of life-history optimization

Craig R. White*, Lesley A. Alton, Candice L. Bywater†, Emily J. Lombardi, Dustin J. Marshall

Organisms use energy to grow and reproduce, so the processes of energy metabolism and biological production should be tightly bound. On the basis of this tenet, we developed and tested a new theory that predicts the relationships among three fundamental aspects of life: metabolic rate, growth, and reproduction. We show that the optimization of these processes yields the observed allometries of metazoan life, particularly metabolic scaling. We conclude that metabolism, growth, and reproduction are inextricably linked; that together they determine fitness; and, in contrast to longstanding dogma, that no single component drives another. Our model predicts that anthropogenic change will cause animals to evolve decreased scaling exponents of metabolism, increased growth rates, and reduced lifetime reproductive outputs, with worrying consequences for the replenishment of future populations.

Metabolism and production (growth and reproduction) affect every aspect of biology, but attempts to understand the relationships between these processes often take very different approaches. Broadly speaking, two schools of thought are applied to understand the interplay between metabolism and biological production (usually growth): metabolic theory and life-history theory. Metabolic theories assume that the exchange or transport of wastes or nutrients across surfaces and through distribution networks constrains patterns of energy allocation to tissue synthesis (*1*–*4*). Metabolism and body size trajectories therefore emerge from these theories as a consequence of assumed physical and chemical constraints on resource acquisition or usage. Life-history theory seeks to understand ontogenetic trajectories through the lens of evolution. It assumes that total resource allocation to survival, growth, and reproduction is limited, and thus allocation to each life-history trait is constrained by trade-offs among traits that have emerged as an outcome of evolutionary selection (*5*, *6*).

Metabolic and life-history theories each have their own strengths and weaknesses. A strength of metabolic theories is that they seek to explore the relationship between metabolism and growth from first principles and are explicit in terms of mass and energy. However, these strengths can also be a weakness if they are applied with a rigid emphasis on the role of intrinsic, absolute constraints without incorporating the capacity of these constraints to evolve in response to selection. A strength of the life-history approach is that it focuses on the ultimate driver of biological production, evolution. An important weakness of this approach is that, for simplicity, overall rates of energy expenditure and net allocation to production are themselves assumed to be evolutionarily inert. It is increasingly clear, however, that metabolism itself is evolutionarily labile and subject to selection (*7*). Here, in contrast to metabolic and life-history theories, we propose that the invocation of constraints is unnecessary to explain the ontogenetic trajectories of metabolism and growth. We explore this idea by modeling how the relationships among metabolism, growth, and reproduction emerge from selection to maximize lifetime reproduction.

Our approach builds on decades of work investigating how metabolism (and its relationship to body mass), growth, and reproduction have coevolved (*8*–*18*). Our approach does not assume that life is unconstrained by physics and chemistry, but instead assumes that there is substantial (and underappreciated) opportunity for evolutionary optimization within these constraints. For example, the evolution of vascular distribution networks has allowed organisms to increase in size beyond the physical and chemical constraints imposed by the slow diffusion of respiratory gases through tissue. Similarly, the large and complex surfaces of lungs, gills, and guts demonstrate how evolution has increased the capacity for exchange of resources beyond the Euclidian geometric constraints imposed by simple surface area-to-volume relationships. Here, we apply that same logic but expand it to consider how whole-organism metabolism might coevolve with the other fundamental components of life: growth and reproduction.

School of Biological Sciences and Centre for Geometric Biology, Monash University, Clayton 3800, Victoria, Australia.
*Corresponding author. Email: craig.white@monash.edu
†Present address: School of Biological Sciences, The University of Queensland, Brisbane 4072, Queensland, Australia.

A model for metabolism, growth, and reproduction

Our model is built upon an energy-expenditure budget for an animal in which the total rate of energy expenditure (E_T) is equal to the sum of the rates of energy allocation to self-maintenance (E_M), production (E_P), digestion (E_D), and activity (E_A). E_P is equal to the sum of the rates of energy allocation to growth (E_G) and reproduction (E_R). All energy expenditure values are expressed as joules per hour. The overhead costs of production continue when an animal is postprandial (i.e., no longer spending energy on digestion) (*19*); therefore, for an inactive postprandial animal when both E_A and E_D are zero,

$$E_T = E_M + E_P = E_M + E_G + E_R \quad (1)$$

The scaling of rates of energy expenditure (metabolic rates) with body mass (m, in grams) is usually well described by a power function $E = a_E m^{b_E}$, where a_E is the scaling coefficient and b_E is the scaling exponent, which is typically <1 for E_T and E_M (*7*, *13*, *20*, *21*) and ≥1 for E_R (*22*, *23*). Following Day and Taylor (*24*), we partitioned total production among growth and reproduction, with allocation to growth occurring early in life and growth ceasing when all of production is allocated to reproduction (e.g., Fig. 1A). Assuming that total production scales allometrically (*24*) with an exponent equal to $b_{E_T} = b_{E_M}$, it follows that animals allocate a fraction (f) of E_T to production [$f = [E_T - E_M]/E_T$)]. Growth rate (in grams per hour) is the change in m over time (t) (dm/dt) and is dictated by E_G and a term that represents the overhead cost of tissue biosynthesis and serves to convert from units of energy to units of mass (C_m, in joules per gram). Before reproductive maturation at size M_{mat}, $E_R = 0$ and all of production is allocated to growth. Growth rate is then calculated by rearranging Eq. 1 to calculate E_G, converting E_G to the mass of tissue synthesized by dividing by C_m, and substituting scaling relationships for E_T as follows:

$$dm/dt = fE_T/C_m = fa_{E_T} m^{b_{E_T}}/C_m \quad (2)$$

After maturation, production is divided among growth and reproduction, and growth rate can be calculated by rearranging Eq. 1 to calculate E_G (i.e., subtracting E_R from f of E_T allocated to E_P) and substituting scaling relationships for both E_T and E_R

$$\begin{aligned} dm/dt &= [fE_T - E_R]/C_m \\ &= \left[fa_{E_T} m^{b_{E_T}} - a_{E_R} m^{b_{E_R}}\right]/C_m \end{aligned} \quad (3)$$

Growth ceases at maximum mass (M, in grams), when all of production is allocated to reproduction (i.e., $fa_{E_T} M^{b_{E_T}} = a_{E_R} M^{b_{E_R}}$), so a_{E_R} can be estimated from f, a_{E_T}, b_{E_T}, b_{E_R},

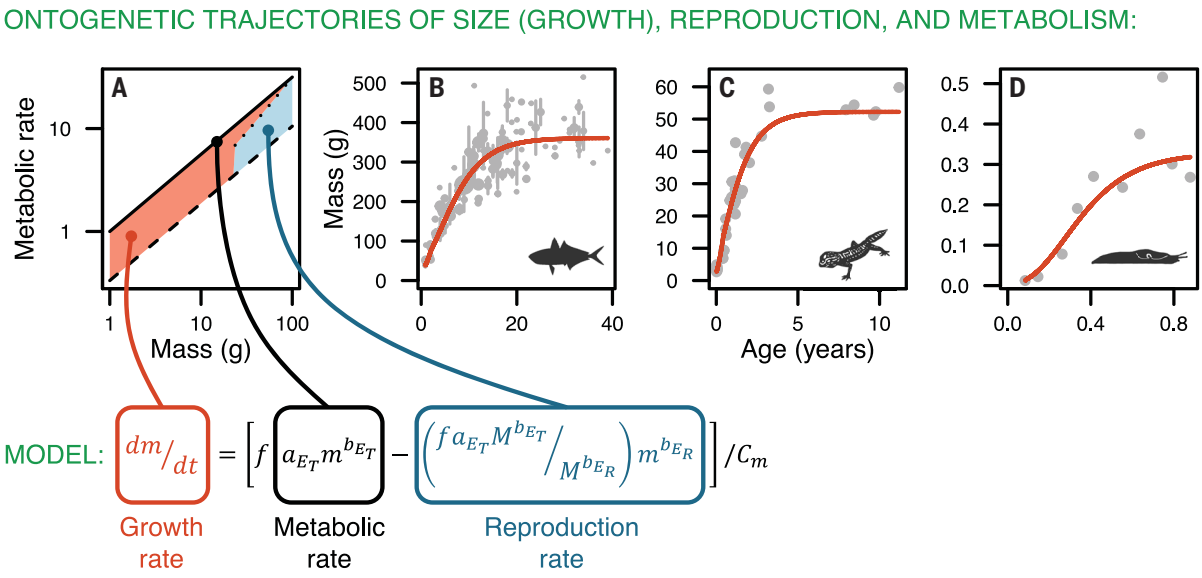

Fig. 1. Division of energy between growth and reproduction yields ontogenetic growth trajectories. (**A**) Size-dependent allocation of energy to production (E_P), which is partitioned among growth (E_G) and reproduction (E_R) and is equal to the difference between total metabolic rate (E_T, solid line) and maintenance metabolic rate (E_M, dashed line). E_R is represented by the blue shaded area bounded by the dotted and dashed lines, and E_G is represented by the red shaded area. (**B** to **D**) Example fits of the growth model to mass-for-age data for Atlantic horse mackerel (B), leopard geckos (C), and gray field slugs (D) (*25*). Error bars in (B) are standard errors for the mean mass of animals of identical age.

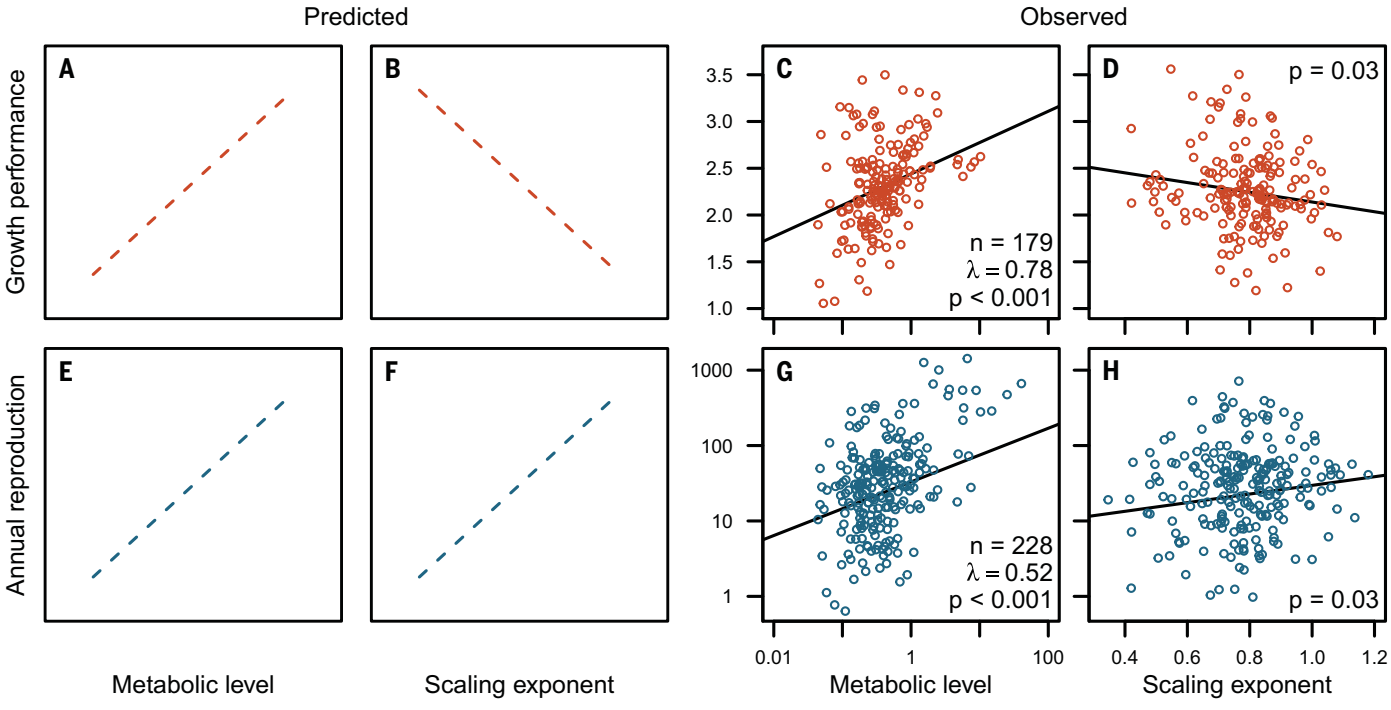

Fig. 2. Life history covaries with metabolic scaling. Predicted and observed effects of metabolic level and the metabolic scaling exponent on growth performance (**A** to **D**) and annual reproduction (**E** to **H**). Metabolic level (*a*, in milliliters of oxygen per hour) and the metabolic scaling exponent (*b*) are estimated from the scaling of metabolic rate (*E*) with mass (*m*) where $E = am^b$. Dashed lines in (A), (B), (E), and (F) depict the directionality of predictions derived from the model described in the text (see fig. S1 for further details). Solid lines in (C), (D), (G), and (H) are empirical relationships estimated from phylogenetic generalized least-squares models including mass and temperature as covariates (tables S1 and S2). Points are shown adjusted for the effects of all other predictors in the model. Phylogenetic heritability (λ) was significantly greater than zero, and the effect of metabolic level and the metabolic scaling exponent was significant for all models (*P* values are shown in the relevant panel, along with sample size, *n*).

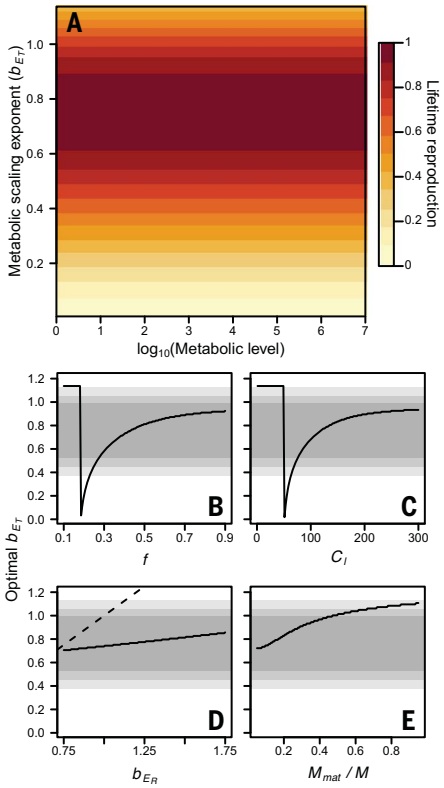

Fig. 3. Allometric scaling of metabolic rate maximizes lifetime reproduction. (**A**) Predicted effects of metabolic level (a_{E_T}, in arbitrary units) and the metabolic scaling exponent (b_{E_T}) on lifetime reproduction (scaled from 0 to 1), where metabolic rate scales with mass (m) as $a_{E_T}m^{b_{E_T}}$. (**B** to **E**) Sensitivity of the optimal value of b_{E_T} (the value that maximizes lifetime reproduction) to variation in key parameters describing growth and reproduction over the life of a hypothetical organism, including: f, the fraction of total metabolism that is allocated to production (growth and reproduction) (B); C_l, a constant linking a_{E_T} with life span (C); b_{E_R}, the scaling exponent of reproductive output (D); and M_{mat}/M, the ratio of mass at maturity to maximum mass (E). Shaded areas in (B) to (E) represent percentile ranges of the empirical distribution of b_{E_T} (Fig. 4), with the darkest shade bounding the 10th and 90th percentiles, the intermediate shade bounding the 5th and 95th percentiles, and the lightest shade bounding the 2.5th and 97.5th percentiles. The dashed line in (D) is the line of unity where $b_{E_T} = b_{E_R}$.

and M by rearrangement. By substituting $a_{E_R} = fa_{E_T}M^{b_{E_T}}/M^{b_{E_R}}$ into Eq. 3 and rearranging, growth rate can be estimated as follows:

$$\frac{dm}{dt} = \frac{f}{C_m} a_{E_T}\left[m^{b_{E_T}} - M^{b_{E_T}}\left(\frac{m}{M}\right)^{b_{E_R}}\right] \quad (4)$$

The integral of Eq. 4 yields a growth trajectory but has no closed-form solution and so must be solved by numerical approximation (e.g., Fig. 1, B to D). Our approach is philosophically similar to that of Day and Taylor (*24*) (e.g., their equation 10) but differs in that we do not fix the scaling exponent of production. Instead, we assume that production is proportional to metabolic rate and set the scaling exponent of production equal to the scaling exponent of metabolic rate. We formulated Eq. 4 using a scaling relationship for reproduction so that it can be easily parameterized using empirical data (e.g., *22*). We note that although the model is formulated for animals that exhibit indeterminate growth, it can also accommodate determinate growth. Determinate growth occurs if animals allocate all of production to reproduction immediately upon reaching maturity (in model terms, determinate growth can arise if the scaling exponents of metabolism and reproduction are equal, or if size at maturity is equal to M).

Conditions that optimize life history

To explore the relationships among metabolic scaling parameters (a_{E_T} and b_{E_T}), growth, and reproduction statistically, it is necessary to derive an estimate of a_{E_T} that is not correlated with b_{E_T}. To do so, we define metabolic level (L) as the metabolic rate estimated at a common mass (m') that results in a correlation of 0 between $\log_{10}L$ and b ($L = a_{E_T}m'^{b_{E_T}}$) (*25*). Defined in this way, L represents a mass-independent estimate of the elevation of the metabolic scaling relationship (i.e., animals with a high L have a high E_T at m'), and b_{E_T} represents the slope of the relationship between $\log_{10}E_T$ and $\log_{10}m$. If the assumptions stated above hold, then Eq. 4 makes four testable predictions, which are illustrated in Fig. 2 and further elaborated in fig. S1: (i) For a given metabolic scaling exponent b_{E_T}, growth will be positively correlated with metabolic level L (Fig. 2A); i.e., animals with a higher metabolic level grow faster [e.g., (*17*, *26*, *27*, *28*)]. (ii) For a given L, growth will be negatively correlated with b_{E_T} (Fig. 2B); i.e., animals with shallower metabolic scaling relationships allocate more energy to production early in life and therefore grow faster. (iii) For a given b_{E_T}, maximum energy allocation to reproduction, $E_{R_{max}}$ (=E_R when $m = M$), will be positively correlated with L (Fig. 2E); i.e., animals with a higher metabolic level allocate more energy to reproduction [e.g., (*29*, *30*)]. (iv) For a given L, $E_{R_{max}}$ will be positively correlated with b_{E_T} (Fig. 2F); i.e., animals that have steeper metabolic scaling relationships allocate more energy to production later in life and therefore have higher maximum reproduction.

To test these four predictions, we compiled intraspecific metabolic scaling and life-history data from the literature and analyzed them in a phylogenetic generalized least-squares framework (*25*). The dataset includes new compilations of ontogenetic scaling relationships expressed as a function of live mass or wet mass, growth trajectories, annual reproduction, and longevity (*31*). We restricted our compilation of growth data to animals that grow after maturation and show growth patterns that are reasonably well approximated by the von Bertalanffy growth equation. We calculated growth performance, a size-independent estimate of growth rate, as Pauly's (*2*) growth performance index (ϕ) from estimates of maximum length (l_∞) and the growth constant (k) derived from fits of von Bertalanffy growth curves to length-at-age data using the equation $\phi = \log_{10}k + 2\log_{10}l_\infty$. Life histories for each species were characterized by mean growth performance, mean annual reproduction, and maximum longevity.

The patterns in the data match all four predictions from Eq. 4: Life histories have been optimized such that growth performance and reproduction both increase with metabolic level (predictions 1 and 3, Fig. 2, C and G), growth performance decreases with the metabolic scaling exponent (prediction 2, Fig. 2D), and reproduction increases with the metabolic scaling exponent (prediction 4, Fig. 2H). The data also show that longevity decreases with metabolic level (fig. S2A), in keeping with the predictions of both metabolic theory (*1*, *10*) and life-history theory (*11*, *32*). Longevity is not related to the metabolic scaling exponent (fig. S2B).

Life-history optimization yields allometric scaling of metabolism

After validating the predictions of our growth model, we next explored the effects of metabolic level and the metabolic scaling exponent to determine whether any combination of these parameters maximizes lifetime reproduction. To do this, we used Eqs. 3 and 4 to generate growth trajectories and estimated lifetime reproduction from the time dependence of m and the scaling of E_R with m for values of m greater than M_{mat}

$$E_R = \left[fa_{E_T}M^{b_{E_T}}/M^{b_{E_R}}\right]m^{b_{E_R}} \quad (5)$$

We used a numerical model to estimate growth and reproduction through 1 million time steps from birth to maximum longevity (*25*). As a first approximation, we modeled animals growing from a starting mass of m = 1 to M = 100 and assumed that b_{E_R} = 1.137 (*22*, *23*) and f = 0.43 (*33*). This estimate of f derived from growth data is broadly consistent with estimates of the energetic cost of egg biomass production in female animals [~50% of basal metabolic rate (*34*)]. The cost of gamete production is lower for males than females (*34*), but costs associated with mating effort can be higher [e.g., (*35*)], and the overall costs associated with reproduction can be similar for males

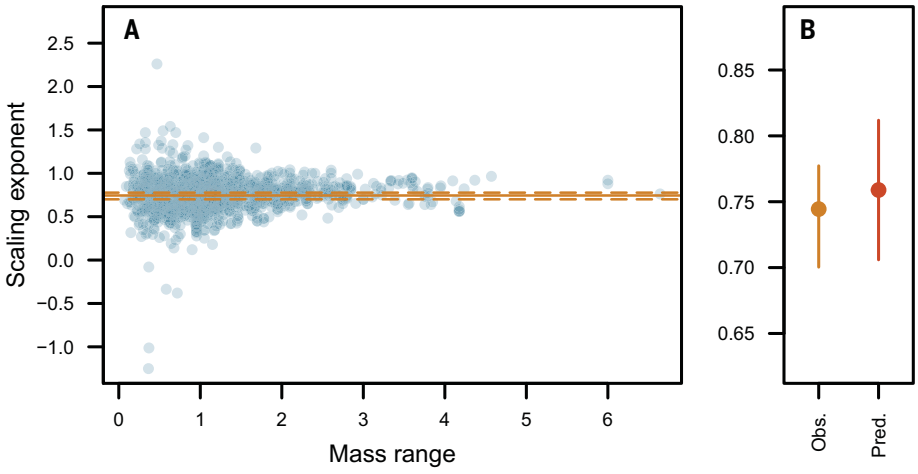

Fig. 4. Metabolic rate scales allometrically with body mass. (**A**) Funnel plot showing the relationship between the intraspecific scaling exponent of metabolic rate and mass range (orders of magnitude) over which the scaling exponent was estimated for scaling exponents estimated from the relationship between metabolic rate and live or wet body mass. The horizontal solid line is the mean of all values (0.743 ± 0.017) estimated in an intercept-only linear mixed model with random intercept terms for species identity and taxonomic group. Dashed lines are the 95% profile likelihood confidence interval (95% CI) for the mean (0.699, 0.777). (**B**) Mean observed scaling exponent (shown ± 95% CI) from the empirical distribution in (A) compared with a scaling exponent predicted to maximize reproduction (Fig. 3A) based on a set of assumptions regarding energy allocation to production, the size dependence of reproduction, size at maturity, and longevity, as described in the text. Plastic or evolutionary changes in energy allocation to production, the size dependence of reproduction, size at maturity, or longevity will yield changes in the scaling exponent predicted to maximize lifetime reproduction (Fig. 3, B to E). The error bars associated with the predicted scaling exponent show the range of values over which lifetime reproduction is >99% of maximum.

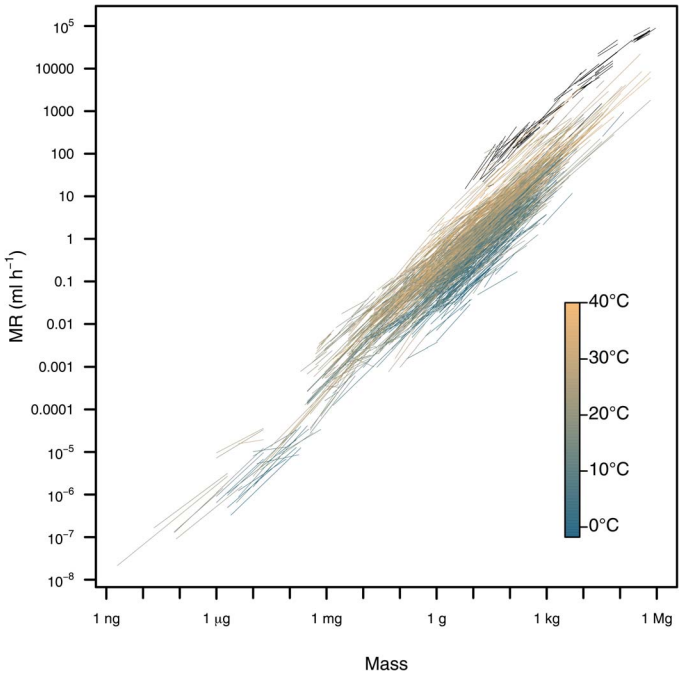

Fig. 5. Scaling of metabolic rate (MR) with body mass. Black lines depict intraspecific scaling relationships for endotherms (birds and mammals). Colored lines depict intraspecific scaling relationships for ectotherms (fishes, amphibians, reptiles, and invertebrates), which are colored by measurement temperature from 1.8° to 40°C.

and females [e.g., (*36*)]. We assumed that M_{mat} = 0.223 M on the basis of data for fish showing that the mean length at maturity is equal to 0.61 of maximum length (*37*) and assuming that, on average, mass is proportional to length cubed. Finally, we assumed that life span is proportional to a constant (C_l) divided by a_{E_T} and first report the results of these analyses with C_l set to an arbitrary value of 120. The value of C_l = 120 was selected because, in combination with the other parameters drawn from data (b_{E_R} = 1.137, f = 0.43, M_{mat} = 0.223 M), this value yields an optimal value of the metabolic scaling exponent (b_{E_T}) that is broadly consistent with the mean value observed in the data (Figs. 3 and 4). We then used sensitivity analyses to explore how variations in the values of b_{E_R}, f, M_{mat}, and C_l alter the optimal value of b_{E_T}.

The model predicts that lifetime reproduction varies with the metabolic scaling exponent b_{E_T} but not with the metabolic level L. Lifetime reproduction is independent of metabolic level over a wide range (Fig. 3A) that far exceeds the approximately three orders of magnitude range of metabolic level observed at any given body mass in the dataset (Fig. 5). Other factors that are not included in our model probably set the upper and lower limits of metabolism at any given size. Such limits may be imposed by resource availability in the environment mediated by minimum viable population sizes (*38*) or by constraints on the capacity of organisms to ingest and process resources or expend energy (*39*).

A key outcome of our study is that the predicted metabolic scaling exponent that maximizes lifetime reproduction is almost always allometric and falls within the range of observed data (Fig. 3; 90% of the observed scaling exponents are <1; Fig. 4A). Our initial parameter estimates for b_{E_R}, f, and M_{mat} were drawn from published data, but the value of C_l was selected to yield an estimate of the optimal scaling exponent of metabolic rate b_{E_T} that closely matches the mean scaling exponent of metabolic rate from the literature compilation, which is ~3/4 (Fig. 4). However, the model does not predict a universally optimal b_{E_T}, but instead predicts that the value of b_{E_T} that maximizes lifetime reproduction depends on the values of f (Fig. 3B), C_l (Fig. 3C), b_{E_R} (Fig. 3D), and M_{mat} (Fig. 3E). The model therefore predicts that evolutionary or plastic changes in energy allocation to production, the size dependence of reproduction, the size at maturity, or the relationship between longevity and metabolism (and thereby production) will yield changes in the scaling of metabolic rate. This is consistent with empirical studies showing that the scaling exponent of metabolic rate varies in response to a wide range of biotic and abiotic variables [e.g., (*12*, *13*, *20*, *21*)].

Our finding that allometric metabolic scaling emerges from the optimization of growth and reproduction within a finite life span to maximize lifetime reproduction offers a potential solution to one of the most enduring controversies in biology (*20*, *21*). Metabolic theories have usually proposed explanations for the allometric scaling of metabolic rate on the basis of the assumption that allometry arises as a consequence of physical geometric constraints, such as those that are imposed by the geometry of resource distribution networks (*3*), the need to dissipate heat produced as a by-product of metabolism (*18*, *39*, *40*), and surface area–to-volume constraints on the fluxes of nutrients or wastes (*1*, *18*). Others have countered that variation in metabolic allometry arises as a consequence of selection rather than constraint [e.g., (*7*, *9*, *12*, *15*, *18*, *21*, *41*–*43*)]. Our model and data support the latter view, that allometric scaling of metabolic rate is predicted to arise if selection optimizes growth and reproduction to maximize lifetime reproduction (Fig. 4). Metabolic allometry can therefore be explained without the need to invoke any of the assumed constraints traditionally imposed by metabolic theories [e.g., (*1*, *4*, *18*, *39*, *40*)].

Allometries are characteristic of life and are observed at the level of enzymes, mitochondria, cells, whole organisms, populations, and ecosystems (*44*–*48*). Kozłowski and colleagues have shown how intraspecific allometries, such as those predicted by our model, yield among-species metabolic scaling patterns that are also allometric (*9*, *41*, *42*). Thus, taken together, the work of Kozłowski and colleagues and our study offer a mathematically explicit explanation for biological allometries at multiple scales of organization. Intraspecific metabolic allometries arise as a consequence of evolutionary optimization of growth and reproduction (Fig. 3), and interspecific metabolic allometries arise as a consequence of evolutionary optimization of body size and metabolic rate [e.g., (*9*, *41*, *42*)]. We therefore suggest that the allometric scaling of metabolic rate arises not because it is inevitable but rather because it is advantageous.

Implications for life histories in the Anthropocene

Elevated extrinsic mortality is a signature of the Anthropocene (*49*). The framework that we provide here not only offers new insight into the origin of biological allometries but also gives us the opportunity to explore and predict how metabolism, growth, and reproduction will respond to future changes in the environment (*25*). Our model predicts that organisms living in a future environment with a 10% increase in mortality (an arbitrary but realistic figure) are predicted to have substantially reduced lifetime reproductive output (–36%) and to evolve lower metabolic scaling exponents (decreased from 0.76 to 0.73) that are associated with more rapid growth and earlier maturation (–1.5%). The substantial decrease in reproduction predicted by the model, and the consequences of this for population replenishment, is particularly concerning.

Conclusion

Our findings suggest that metabolism, growth, and reproduction have coevolved to maximize fitness (i.e., lifetime reproduction) and that the observed patterns in these fundamental characteristics of life can be explained by optimization rather than constraint. We offer this as an alternative way of viewing the origin of biological allometries at all scales, recognizing that it represents a profound departure from classic thinking. Our viewpoint is analogous to the concept of the Hutchinsonian niche (*50*): Constraints define the range within which life is possible (analogous to the fundamental niche), whereas optimization yields the (smaller) range of possibilities exploited by life (analogous to the realized niche). We reiterate that this viewpoint does not deny the existence of biophysical constraints and does not call forth Darwinian demons (hypothetical organisms that maximize all aspects of fitness simultaneously and would exist if there were no constraints on evolution). Rather, our approach expands the phenotypic space in which evolutionary optimization operates and avoids giving primacy of causation to any single pillar of multicellular life. It also emphasizes that the pillars of metabolism, growth, and reproduction have coevolved to shape each other, and, consequently, observed life-history strategies emerge from the optimization of these to maximize lifetime reproduction within a finite life span (*8*, *9*, *15*, *41*, *42*). Within this multivariate optimization dwells the great diversity of life histories in nature.

REFERENCES AND NOTES

1. S. A. L. M. Kooijman, *Dynamic Energy Budget Theory for Metabolic Organisation* (Cambridge Univ. Press, ed. 3, 2010).
2. D. Pauly, "Gill size and temperature as governing factors in fish growth: A generalization of von Bertalanffy's growth formula" (Institut fur Meereskunde, 1979); https://agris.fao.org/agris-search/search.do?recordID=AV2012092482.
3. G. B. West, J. H. Brown, B. J. Enquist, *Nature* **413**, 628–631 (2001).
4. M. R. Kearney, *Biol. Rev. Camb. Philos. Soc.* **96**, 557–575 (2021).
5. A. J. Zera, L. G. Harshman, *Annu. Rev. Ecol. Syst.* **32**, 95–126 (2001).
6. S. C. Stearns, *Funct. Ecol.* **3**, 259 (1989).
7. C. R. White *et al*., *Nat. Ecol. Evol.* **3**, 598–603 (2019).
8. R. H. Peters, *Cambridge Studies in Ecology: The Ecological Implications of Body Size* (Cambridge Univ. Press, 1986).
9. J. Kozłowski, J. Weiner, *Am. Nat.* **149**, 352–380 (1997).
10. J. H. Brown, J. F. Gillooly, A. P. Allen, V. M. Savage, G. B. West, *Ecology* **85**, 1771–1789 (2004).
11. J. R. Speakman, *J. Exp. Biol.* **208**, 1717–1730 (2005).
12. D. S. Glazier *et al*., *Ecol. Monogr.* **81**, 599–618 (2011).
13. S. S. Killen, D. Atkinson, D. S. Glazier, *Ecol. Lett.* **13**, 184–193 (2010).
14. I. A. Hatton, A. P. Dobson, D. Storch, E. D. Galbraith, M. Loreau, *Proc. Natl. Acad. Sci. U.S.A.* **116**, 21616–21622 (2019).
15. D. S. Glazier, *Biol. Rev. Camb. Philos. Soc.* **90**, 377–407 (2015).
16. D. S. Glazier, *Systems* **2**, 451 (2014).
17. S. Wong, J. S. Bigman, N. K. Dulvy, *Proc. Biol. Sci.* **288**, 20210910 (2021).
18. D. S. Glazier, *Biol. Rev. Camb. Philos. Soc.* **85**, 111–138 (2010).
19. J. Rosenfeld, T. Van Leeuwen, J. Richards, D. Allen, *J. Anim. Ecol.* **84**, 4–20 (2015).
20. C. R. White, M. R. Kearney, *Compr. Physiol.* **4**, 231–256 (2014).
21. D. S. Glazier, *Biol. Rev. Camb. Philos. Soc.* **80**, 611–662 (2005).
22. D. R. Barneche, D. R. Robertson, C. R. White, D. J. Marshall, *Science* **360**, 642–645 (2018).
23. D. J. Marshall, C. R. White, *Trends Ecol. Evol.* **34**, 102–111 (2019).
24. T. Day, P. D. Taylor, *Am. Nat.* **149**, 381–393 (1997).
25. Materials and methods are available online in the supplementary materials.
26. T. J. Case, *Q. Rev. Biol.* **53**, 243–282 (1978).
27. R. Ton, T. E. Martin, *Funct. Ecol.* **30**, 743–748 (2016).
28. J. M. Grady, B. J. Enquist, E. Dettweiler-Robinson, N. A. Wright, F. A. Smith, *Science* **344**, 1268–1272 (2014).
29. B. K. McNab, *Physiological Ecology of Vertebrates* (Comstock Cornell, 2002).
30. D. S. Glazier, *Comp. Biochem. Physiol. A Comp. Physiol.* **80**, 587–590 (1985).
31. C. R. White, L. A. Alton, C. L. Bywater, E. J. Lombardi, D. J. Marshall, Metabolic scaling, growth, and reproduction data for animals for: Metabolic scaling is the product of life-history optimization, Zenodo (2022); https://doi.org/10.5281/zenodo.6782436.
32. R. E. Ricklefs, M. Wikelski, *Trends Ecol. Evol.* **17**, 462–468 (2002).
33. P. Rombough, in *Comparative Developmental Physiology: Contributions, Tools, and Trends*, S. J. Warburton, W. W. Burggren, B. Pelster, C. L. Reiber, J. Spicer, Eds. (Oxford Univ. Press, 2006), pp. 99–123.
34. A. Hayward, J. F. Gillooly, *PLOS ONE* **6**, e16557 (2011).
35. M. J. Chung, M. D. Jennions, R. J. Fox, *Evol. Lett.* **5**, 315–327 (2021).
36. J. E. Lane, S. Boutin, J. R. Speakman, M. M. Humphries, *J. Anim. Ecol.* **79**, 27–34 (2010).
37. A. C. Tsikliras, K. I. Stergiou, *Rev. Fish Biol. Fish.* **24**, 219–268 (2014).
38. R. Lande, *Am. Nat.* **142**, 911–927 (1993).
39. J. R. Speakman, E. Król, *J. Anim. Ecol.* **79**, 726–746 (2010).
40. R. Sarrus, N. Rameaux, *Méd.* **3**, 1094 (1839).
41. J. Kozłowski, M. Konarzewski, A. T. Gawelczyk, in *Macroecology: Concepts and Consequences*, T. M. Blackburn, K. J. Gaston, Eds. (Blackwell Science, 2003), pp. 299–320.
42. J. Kozłowski, M. Konarzewski, M. Czarnoleski, *Biol. Rev. Camb. Philos. Soc.* **95**, 1393–1417 (2020).
43. P. A. C. L. Pequeno, F. B. Baccaro, J. L. P. Souza, E. Franklin, *Ecol. Entomol.* **42**, 115–124 (2017).
44. G. N. Somero, J. J. Childress, *J. Exp. Biol.* **149**, 319–333 (1990).
45. J. Damuth, *Biol. J. Linn. Soc. Lond.* **31**, 193–246 (1987).
46. V. M. Savage, J. F. Gilloly, J. H. Brown, E. L. Charnov, *Am. Nat.* **163**, 429–441 (2004).
47. A. P. Allen, J. F. Gillooly, J. H. Brown, *Funct. Ecol.* **19**, 202–213 (2005).
48. G. B. West, W. H. Woodruff, J. H. Brown, *Proc. Natl. Acad. Sci. U.S.A.* **99** (suppl. 1), 2473–2478 (2002).
49. S. P. Otto, *Proc. Biol. Sci.* **285**, 20182047 (2018).
50. G. E. Hutchinson, *Cold Spring Harb. Symp. Quant. Biol.* **22**, 415–427 (1957).

ACKNOWLEDGMENTS

C.R.W. is grateful for more than 20 years of discussions on the topic of biological allometry with R. Seymour, who provided comments on an earlier version of this manuscript. We also acknowledge J. Kozłowski's essential role in shaping our thinking on this topic. **Funding:** This work was supported by the Australian Research Council (grants DP180103925 and DP220103553).
Author contributions: Conceptualization: C.R.W., D.J.M.; Formal analysis: C.R.W.; Funding acquisition: C.R.W., L.A.A.; Investigation: C.R.W., L.A.A., C.L.B., E.J.L.; Methodology: C.R.W., D.J.M.;

Writing – original draft: C.R.W., L.A.A., D.J.M.; Writing – review & editing: C.R.W., L.A.A., C.L.B., E.J.L., D.J.M. **Competing interests:** The authors declare no competing interests. **Data and materials availability:** The data needed to reproduce the results described in this study are hosted at Zenodo (*31*). **License information:**

SUPPLEMENTARY MATERIALS

science.org/doi/10.1126/science.abm7649
Materials and Methods
Figs. S1 and S2
Tables S1 to S3
References (*51*–*73*)
MDAR Reproducibility Checklist

Submitted 10 October 2021; resubmitted 16 March 2022
Accepted 8 July 2022
10.1126/science.abm7649